

**INVESTIGATION ON NASAL AIRFLOW OF  
MALAYSIAN FEMALES USING CFD**

**LEE CHIH FANG**

**UNIVERSITI SAINS MALAYSIA**

**2014**

## **Acknowledgement**

Upon the completion of this research, I have received plenty of help from my lecturers, technicians, family and friends. First and foremost, I would like to take this opportunity to express my sincere appreciation and gratitude to my supervisor, Prof. Mohd. Zulkifly Bin Abdullah, for his suggestions, guidance and efforts to ensure the successful completion of this research. I would like to thank my co-supervisor as well, Assoc. Prof. Dr. Kamarul Arifin Bin Ahmad for introducing this research to me and build my interest into this field. Thanks for every meeting sessions spent troubleshooting my analysis problems and the constant monitoring of my progress despite their busy schedules.

In addition to that, I would like to thank my co-supervisor, Prof. Ibrahim Lutfi Bin Shuaib from Advanced Medical and Dental Institute, USM, Kepala Batas for giving me the required data that are crucial in order for me to carry out this research. Without all the raw data, it is impossible for me to start my research. I really appreciate their help for giving me their important point of views from medical side as I, from an engineering background are lacking of those explanations. Thanks for answering all my enquiries especially regarding all the medical terms and its explanation, and giving me the confirmation and confidence in what I am doing will be beneficial in both engineering and medical world. Not forgotten, thanks to both my co-supervisors, Dr. Rushdan Bin Ismail and Assoc. Prof. Dr. Suzina Sheikh Abdul Hamid from School of Medical Sciences, Health Campus, USM, Kubang Kerian for their guidance and support throughout this research. Special thanks to all technicians from School of Aerospace Engineering for giving me their full cooperation and lending their helpful hands throughout the entire research period especially during experimental works.

Finally, I would like to extend my gratitude to all the parties involved directly or indirectly in helping me complete this research. Last but not least, my deepest appreciation to my beloved family and friends for their full support, encouragement and patience during the entire research period.

## **TABLE OF CONTENTS**

Acknowledgement	ii
Table of Contents	iv
List of Tables	x
List of Figures	xii
Abstrak	xvii
Abstract	xix
CHAPTER 1 – INTRODUCTION	
1.1 Research Background	1
1.2 Problem Statement	3
1.3 Aims and Objectives	6
1.4 Scope of Work	6
1.5 Thesis Organization	9
CHAPTER 2 – LITERATURE REVIEW	
2.1 Nasal Anatomy	11
2.1.1 Nasal Structures and Functions	11
2.2 Mucous and Related Fields	15

2.2.1	Mucus Characteristics and Structures	16
2.2.2	Nasal Mucociliary Clearance	19
2.3	Computational Analysis	20
2.3.1	Geometrical Modelling	21
2.3.2	Advantages of Computational Simulations	24
2.4	Experimental Studies	26
2.4.1	Experimental Model	27
2.4.2	Experimental Set-up	29
2.4.3	Seeding Particles	31
2.5	Objective Measurement Methods	33
2.6	Standardized/Averaged Models	35
2.7	Disease Cases	37
2.8	Summary	39
	CHAPTER 3 – METHODOLOGY	42
3.1	Flow Chart	42
3.2	Computational Analysis	45
3.2.1	Construction of Geometry	46

3.2.1.1	Individual Nasal Model	46
3.2.1.2	Standardized Nasal Model	49
3.2.1.3	Half Nasal Model	56
3.2.2	Meshing of Geometry	57
3.2.2.1	Grid Independence Study and Grid Quality	58
3.2.3	Running Analysis	66
3.2.3.1	Solution Parameters	66
3.2.3.2	Solution	71
3.3	Experimental Works	74
3.3.1	Fabrication of Experimental Model	74
3.3.2	Experimental Set-Up	76
3.3.3	Selection of Seeding Particles	79
3.4	Acoustic Rhinometry	80
CHAPTER 4 – RESULTS AND DISCUSSIONS		82
4.1	Verification and Validation	82
4.1.1	Verification	83
4.1.2	Validation	85
4.1.2.1	Acoustic Rhinometry	87

4.1.2.2	Experimental Comparisons	88
4.1.2.3	Computational Comparisons	91
4.2	Mucous Layer Effects	93
4.2.1	Laminar Airflow Simulations	94
4.2.1.1	Velocity Streamlines	94
4.2.1.2	Average Velocity Magnitude	96
4.2.1.3	Maximum Velocity	98
4.2.2	Turbulent Airflow Simulations	100
4.2.2.1	Velocity Streamlines	100
4.2.2.2	Average Velocity Magnitude	102
4.2.2.3	Maximum Velocity	104
4.3	Standardized Nasal Cavity	105
4.3.1	Inspiration and Expiration	106
4.3.1.1	Inspiration	107
4.3.1.2	Expiration	112
4.3.2	Comparisons with Standardized Model	117
4.3.2.1	Cross Sectional Areas	117

4.3.2.2	Average Velocity Magnitudes	120
4.3.2.3	Contours of Velocities	121
4.3.3	Comparisons with Individual Models	124
4.3.3.1	Cross Sectional Areas	124
4.3.3.2	Average Velocity Magnitudes	126
4.3.3.3	Contours of Velocities	127
4.3.4	Comparisons with Previous Works	130
4.3.4.1	Cross Sectional Areas	130
4.3.4.2	Pressure Drop	135
4.4	Disease Cases	137
4.4.1	Geometrical Comparisons	141
4.4.2	Cross Sectional Areas	145
4.4.3	Average Velocity Magnitudes	146
4.4.4	Velocity Contours	150
4.5	Summary	157
CHAPTER 5 – CONCLUSION AND FUTURE RECOMMENDATIONS		159
5.1	Conclusion	159



5.2	Future Recommendations	162
	References	165
	List of Publications	183

## List of Tables

Table 2.1: Experimental set-up.....	33
Table 3.1: Table of information for 26 female subjects used in generation of standardized nasal model.....	51
Table 3.2: Grid qualities of different densities mesh for non-mucous models.....	60
Table 3.3: Grid quality of individual models with different mucous layer thickness	61
Table 3.4: Grid qualities of standardized half model and Liu et al.'s model.....	62
Table 3.5: Grid qualities of standardized model.....	64
Table 3.6: Grid qualities of selected standardized model and four individual female models.....	66
Table 3.7: Reynolds number calculated for nasal models.....	72
Table 3.8: Properties of acrylic (Accura ClearVue Material) .....	75
Table 3.9: Conversion of air flow rate to mixture flow rate.....	78
Table 3.10: Seeding particles.....	79
Table 4.1: Verification.....	85
Table 4.2: Validation.....	86
Table 4.3: Contours of velocities for both models (125 ml/s) .....	123
Table 4.4: Contours of velocities for mass flow rate of 125 ml/s.....	129
Table 4.5: Length of nasal cavities.....	133

Table 4.6: CT scans of healthy and disease nasal cavities.....	140
Table 4.7 : Three dimensional models of the standardized model and pre and post- operation for patient A and patient B.....	144
Table 4.8: Inspiration velocity contours for standardized model, pre and post- operation of patient A and patient B (125 ml/s) .....	152
Table 4.9: Expiration velocity contours for standardized model, pre and post- operation of patient A and patient B (125 ml/s) .....	155
Table 4.10: Inspiration velocity vectors and streamlines for standardized model, patient A and B (300 ml/s) .....	156

## List of Figures

Figure 2.1: Nose anatomy (a) CT scan - Axial view, (b) CT scan – Coronal view, (c) 3D view of nasal cavity and (d) Half nasal cavity with labels .....	12
Figure 2.2 : Human paranasal sinuses: (1) Frontal, (2) Ethmoidal, (3) Maxillary and (4) Sphenoidal (Figure obtained from (Kunkel et al., 2009)) .....	15
Figure 2.3: Ultrastructure of the nasal wall at the respiratory region that shows the pseudo-stratified columnar and ciliated epithelium, the mucus producing goblet cells, the lamina propria, the mucous and serous glands and the cavernous sinusoids (Figures obtained from (Elad et al., 2008) and Slomianka, 2006)) .....	18
Figure 2.4: Models of the nasal cavity (a) Anatomically identical model, (b) Nasal cavity with additional inlet tube and extended nasopharynx, and (c) Simplified nose-like model (Figures obtained from (Shi et al., 2006) and (Elad et al., 2008)) .....	23
Figure 2.5: (a) Transparent model from Hopkins et al.(Hopkins et al., 2000) and (b) Transparent model from (Garcia et al., 2007b) .....	28
Figure 2.6: Experimental set-up (Obtained from (Spence et al., 2011a)) .....	30
Figure 2.7: (a) Acoustic rhinometry and (b) Active anterior rhinomanometry (Figure obtained from (Thulesius, 2012)) .....	35
Figure 3.1: Simplified flow chart .....	43
Figure 3.2: Two-dimensional CT scans (a) Axial, (b) Coronal, (c) Sagittal and (d) Overall views for individual nasal model in MIMICS .....	47
Figure 3.3: (a) Front and (b) Side view of individual nasal cavity .....	48
Figure 3.4: Polylines for individual nasal model created from MIMICS .....	48
Figure 3.5: Three-dimensional individual nasal cavity.....	48

Figure 3.6: (a) Cropping image, (b) Rotating image and (c) Average image obtained .....	54
Figure 3.7: Creation standardized nasal model in MIMICS (a) Axial, (b) Coronal, (c) Sagittal and (d) Three-dimensional views.....	55
Figure 3.8: Standardized model (a) Polylines from MIMICS and (b) Smooth 3D standardize nasal model from CATIA .....	55
Figure 3.9: Half nasal models (a) Model obtained from (Liu et al., 2009) and (b) Standardized model.....	56
Figure 3.10: Three-dimensional nasal model imported to GAMBIT .....	57
Figure 3.11: Velocity magnitudes for non-mucous model (Mass flow rate = 7.5 L/min).....	60
Figure 3.12: Velocity magnitudes for standardized half model .....	63
Figure 3.13: Velocity magnitudes for standardized model (Mass flow rate = 7.5 L/min).....	65
Figure 3.14: (a) Smooth identical geometry obtained after clean up processes and ..	69
Figure 3.15: Four different locations of cutting planes (A = Vestibule, B = Nasal valve, C = Middle plane and D = Nasopharynx) .....	73
Figure 3.16: Left and right cutting planes .....	73
Figure 3.17: CATIA model of 2.5 times larger in scale .....	76
Figure 3.18: Final product of experimental model .....	76
Figure 3.19: (a) Location of camera and (b) Nasal model inside Plexiglass box.....	77
Figure 3.20: (a) Photograph and (b) Schematic diagram of the experimental set-up.	78

Figure 3.21: Schematic diagram of acoustic rhinometry (Figure obtained from (Roithmann et al., 1995)) .....	81
Figure 4.1: Cross sectional areas obtained from acoustic rhinometry and computational measurements .....	88
Figure 4.2: (a) Computational velocity vectors and (b) Experimental velocity vectors of the flow entering the nasal cavity .....	90
Figure 4.3: (a) Computational velocity vectors and (b) Experimental velocity vectors of the flow exiting the nasal cavity .....	90
Figure 4.4: Pressure drop versus mass flow rate .....	92
Figure 4.5: Average velocity comparisons for mass flow rate of (a) 125 ml/s and (b) 250 ml/s .....	93
Figure 4.6: Velocity streamlines (m/s) of mass flow rate (a) 7.5 L/min and .....	96
Figure 4.7: Graphs of average velocity magnitudes (m/s) versus thickness of mucous layer ( $\mu\text{m}$ ) at four cutting planes for mass flow rate of (a) 7.5 L/min and (b) 10 L/min .....	97
Figure 4.8: Percentage of difference for average velocity magnitude at mass flow rate of (a) 7.5 L/min and (b) 10 L/min.....	98
Figure 4.9: Graphs of maximum velocity (m/s) versus mucous layer thickness ( $\mu\text{m}$ ) at four cutting planes for mass flow rate of (a) 7.5 L/min and (b) 10 L/min .....	99
Figure 4.10: Percentage of difference for maximum velocity at mass flow rate of (a) 7.5 L/min and (b) 10 L/min .....	99
Figure 4.11: Velocity streamlines of mass flow rate (a) 15 L/min and (b) 20 L/min .....	102

Figure 4.12: Graphs of average velocity magnitudes (m/s) versus thickness of mucous layer ( $\mu\text{m}$ ) at four cutting planes for mass flow rate of (a) 15 L/min and ..	103
Figure 4.13: Percentage of difference for average velocity magnitude at mass flow rate of (a) 15 L/min and (b) 20 L/min .....	103
Figure 4.14: Graphs of maximum velocity (m/s) versus mucous layer thickness ( $\mu\text{m}$ ) at four cutting planes for mass flow rate of (a) 15 L/min and (b) 20 L/min .....	105
Figure 4.15: Percentage of difference for maximum velocity at mass flow rate of ..	105
Figure 4.16: Location of circulation during inspiration (Figure obtained from (Hörschler et al., 2003) .....	108
Figure 4.17: Inspiration velocity streamlines and velocity vectors (a and b) 125 ml/s and (c and d) 400 ml/s .....	109
Figure 4.18: Inspiration velocity contours and pressure contours (a and c ) 125 ml/s and (b and d) 400 ml/s .....	111
Figure 4.19: Expiration velocity streamlines and velocity vectors (a and c ) 125 ml/s and (b and d) 400 ml/s .....	114
Figure 4.20: Streamlines for expiration obtained from (Chung and Kim, 2008) .....	115
Figure 4.21: Expiration velocity contours and pressure contours (a and c ) 125 ml/s and (b and d) 400 ml/s .....	116
Figure 4.22: Half models (a) Model from current study, Model A and (b) Model obtained from Liu et al., Model B. Cutting planes: A=Vestibule, B=Nasal valve, C=Plane 1, D=Plane 2, E=Middle Plane, F=Plane 3, G=Plane 4 and H=Nasopharynx .....	119
Figure 4.23: Cross sectional areas along nasal cavities .....	120

Figure 4.24: Graph of average velocity magnitudes at four cross sections (125 ml/s)	121
Figure 4.25: Cross sectional area comparisons of Model A and other 4 models	125
Figure 4.26: Graphs of average velocity magnitude at four cross sections along the nasal cavities	126
Figure 4.27: Graphs of maximum velocities at four cross sections along the nasal cavities	127
Figure 4.28: Location of cutting planes used for comparisons with previous works	131
Figure 4.29: Cross sectional areas of full model (both cavities) versus axial distance	131
Figure 4.30: Cross sectional areas for half model (right side) versus axial distance	135
Figure 4.31: Pressure drop versus mass flow rate	137
Figure 4.32: Graphs of cross sectional areas for standardized model, patient A and patient B (pre and post-operation) along the nasal cavities	146
Figure 4.33: Average velocity magnitudes along the nasal cavities for mass flow rate of 125 ml/s	148
Figure 4.34: Average velocity magnitudes along the nasal cavities for mass flow rate of 300 ml/s	148
Figure 4.35: Average velocity magnitude for (a) 125 ml/s and (b) 300 ml/s	150



# **PENYELIDIKAN PEREDARAN UDARA DI DALAM RONGGA HIDUNG PEREMPUAN MALAYSIA MENGGUNAKAN CFD**

## **ABSTRAK**

Kegagalan kaedah pengukuran objektif dalam mendapatkan maklumat penting berkenaan aliran udara di dalam rongga hidung manusia menjurus kepada penggunaan Pengkomputeran Dinamik Bendalir (CFD) untuk mengkaji serta menganalisis struktur rongga hidung yang rumit. Kajian ini hanya memberi tumpuan kepada penyiasatan terperinci terhadap rongga hidung wanita Malaysia yang melibatkan kesan lapisan bendalir mukus, model purata standard dan juga kajian terhadap penyakit sinusitis. Dalam kajian ini, kesan lapisan bendalir mukus terhadap aliran udara di dalam rongga hidung dijalankan dengan penebalan lapisan mukus dari 5 hingga 50  $\mu\text{m}$  dan analisis dijalankan dengan kadar aliran udara antara 7.5 hingga 20 L/min. Keputusan analisis rongga hidung tanpa lapisan bendalir mukus dibandingkan dengan keputusan analisis rongga hidung dengan pelbagai ketebalan lapisan mukus. Berdasarkan keputusan yang diperolehi, lapisan mukus yang sihat iaitu dengan ketebalan 5 hingga 30  $\mu\text{m}$  tidak memberikan sebarang kesan terhadap keseluruhan aliran udara di dalam rongga hidung. Rongga hidung manusia mempunyai ciri-ciri yang unik dan tersendiri dan ini menyebabkan kajian ini menghasilkan satu model purata standard. Metodologi yang digunakan dalam kajian ini melibatkan “programming” ringkas untuk mendapatkan purata pixel daripada set imej Tomographi Berkomputer (CT). Oleh itu, kaedah ini lebih mudah dan hanya memerlukan tempoh masa yang singkat berbanding dengan kaedah yang lain. Purata magnitud kelajuan yang diperolehi daripada pengiraan empat model individual menunjukkan persamaan dengan model standard dan perbezaan antara kedua-duanya

ialah kurang daripada 20%. Ini membuktikan bahawa model purata standard mampu mewakili rongga hidung standard populasi perempuan Malaysia. Perbezaan yang ketara daripada perbandingan dengan model standard dari populasi lain menunjukkan bahawa model standard bagi pelbagai populasi adalah diperlukan kerana kepelbagaian bentuk rongga hidung manusia. Di samping itu, eksperimen Pengimejan Kelajuan Partikel (PIV) dan ukuran akustik rinometri dijalankan bagi tujuan pengesahan. Persamaan daripada perbandingan antara kaedah pengkomputeran, pengiraan, experiment dan juga ukuran rinometri menjadi pengesahan yang kukuh bagi analisis yang dijalankan dalam kajian ini. Sebagai langkah pertama dalam melibatkan penggunaan kaedah pengkomputeran dalam pembedahan maya pada masa hadapan, kajian ini menganalisis imej-imej CT dua pesakit wanita (resdung) sebelum dan juga selepas menjalankan pembedahan. Analisis CFD sebelum dan selepas pembedahan membolehkan pemerhatian yang lebih baik terhadap tempat jangkitan dan juga aliran udara seperti kelajuan bagi pakar rhinologi melihat kesan daripada pembedahan tersebut. Hasil pemerhatian dan keputusan yang diperolehi dari kajian ini mampu membawa kepada kemajuan pembedahan maya serta memberi manfaat kepada pembangunan penyelidikan klinikal.

# **INVESTIGATION ON NASAL AIRFLOW OF MALAYSIAN FEMALES USING CFD**

## **ABSTRACT**

Inabilities of objective measurement methods to obtain various important information regarding human nasal airflow leads to the application of Computational Fluid Dynamics (CFD) to study and analyze the complicated structures of the nasal cavity. This research focuses on detailed investigation of Malaysian female nasal cavities which includes mucous effects, standardized model and disease cases. In this study, mucous layer effects on nasal airflow were studied by thickening the mucous layer from 5 to 50  $\mu\text{m}$  and analysis were carried out with mass flow rate ranging from 7.5 to 20 L/min. Analysis results of non-mucous effects were compared with the thickening mucous layer effects. Based on the results obtained, healthy mucous layer thickness within the range of 5 to 30  $\mu\text{m}$  caused insignificant effects towards the total nasal airflow. Unique and distinctive features of the human nasal cavities require generalization of its geometry and thus, this study creates a standardized female Malaysian nasal cavity. The methodology implemented in this research involves simple programming of averaging pixel values from a set of Computational Tomography (CT) scans. Therefore, it is simpler and requires shorter time compared to other method used in previous research. The average velocity magnitudes calculated from the four individual models match closely with the standardized model with a difference of less than 20%. This proves that the generated model can represent an average and standardized model of an adult Malaysian female. Huge differences from the comparisons with the standardized model of different population shows the need for a standardized model which represents different

population due to the diversity of the human nasal cavities. In addition to that, Particle Image Velocimetry (PIV) experimental work and acoustic rhinometry measurements were carried out for validation purposes. Good agreement between the computational, calculation, experimental and rhinometry measurements results provides a strong validation of the computational analysis conducted in this research. As an initial step towards implementing virtual surgery in the future, this study analyzed the pre-operation and post-operation CT scans of the two female patients with nasal diseases (sinusitis). CFD analysis for pre and post-operation conditions allow better observation of the infected areas as well as the nasal airflow behavior such as velocity magnitudes in order to assist rhinologist to view the effects of the surgeries carried out. The results and observations obtained from this research bring a step forward in advancement of virtual surgery in the future and will be beneficial in clinical research development.

# **CHAPTER 1 – INTRODUCTION**

## **1.1 – Research Background**

This research is focused on the computational modelling of nasal airflow and the implementation of Computational Fluid Dynamics (CFD) in various studies such as the effects of mucous layers, standardized model and disease cases. CFD has been widely used to study the nasal airflow which is difficult to be carried out via objective measurement methods due to the complex structure of the nose. Based on previous works, CFD has been proven to be reliable and provides plenty of advantages in obtaining important information on nasal airflow. A better understanding of the nose physiology, patho-physiology of normal breathing and the post-processing techniques of the flow patterns between left and right nasal cavities can be achieved using CFD (Wen et al., 2008, Zachow et al., 2007, Wen et al., 2007). In this work, CFD involves three-dimensional geometrical modelling, meshing of geometry and running analysis.

The human nasal cavity consists of two nearly symmetrical complex three-dimensional nasal passages which are separated in the middle by the nasal septum. During inspiration, air flows into the nasal cavity from the nostrils reaches the smallest cross sectional region, the nasal valve before reaching the tortuous turbinates region that forms large cross sectional areas covered with mucous layers and cilia. These moist regions play an important role for the humidification, warming and cleansing of the inspired air by entrapping the air-borne particles as well as moistening the air via evaporation (Garcia et al., 2007a). Mucous layer is made up of epithelium and lamina propria, varies in thickness, type of epithelial, characteristics according to its location and its function in the nose (Franks, 2005). Any alteration to

the mucous layer exceeding certain limits induces a negative impact in maintaining an unobstructed nasal airflow.

(Doorly et al., 2008a) suggested that the establishment of rational methods to characterize and compare different anatomies would be very helpful in future studies. There is no guideline or benchmark that can be used as a reference when comparing the various results obtained. Therefore, this leads to the creation of a standardized model that will be used to represent a certain population. (Liu et al., 2009) developed a method to scale, orientate and align the nasal geometries of 30 sets of CT scans of healthy subjects. The research also mentioned the importance of a standardized model for future experimental and numerical studies of inhaled aerosols. Experimental approaches were also implemented for the investigation of airflow in healthy and pathological cases using Particle Image Velocimetry (PIV) (Kim and Haw, 2004, Kim and Son, 2003, Garcia et al., 2007b, Kim and Son, 2004, Kim and Chung, 2009, Kim and Chung, 2004). (Spence et al., 2011b) carried out experimental works via stereoscopic PIV measurements to study the flow in the nasal cavity with high flow therapy.

Various disease cases have been investigated to understand the nature of the diseases and finding the cure to lessen the pains bared by patients. Improvement in radiographic imaging also helps in the diagnosis of chronic sinusitis as using a limited CT scans is a better option for initial evaluation of the disease (Garcia et al., 1994). (Garcia et al., 2007a) proposed that excessive evaporation of the mucous layer is the cause of atrophic rhinitis and comparisons were carried out for both pre and post-operation with a healthy model created from the averaging of four healthy models. In order to obtain vital information for any treatment methods, healthy cases are required for comparison purposes (Weinhold and Mlynski, 2003).

CFD studies on the disease cases will give better perceptives for treatment planning in the future.

## **1.2 – Problem Statement**

The complex structure of human nasal cavity causes difficulties for direct measurement methods to obtain certain information related to nasal airflow. The most popular objective techniques for measurement of nasal function, which are acoustic rhinometry and rhinomanometry, still render ambiguities and inconsistencies in the results obtained (Wolf et al., 2004). The application of CFD in biomedical researches has been proven to have its advantages and therefore allows more studies to be carried out on human nasal cavity. (Zuber, 2012) investigated the nasal physiology and roles of several anatomical features such as turbinates and nasal valve inside the nasal cavity. Other than that, (Zuber, 2012) also performed PIV experimental works for validation and also carried out studies to compare the pre and post-operative data obtained from simulations. This research is a continuation of work carried out by Zuber.

Various assumptions made in previous studies related to nasal airflow have caused changes in the real anatomical nose model and the influence of mucous layer in studies of the nasal airflow is neglected. Furthermore, no effort has been made to alter images by intentionally thickening or manipulating the surface to represent the possible soft tissue displacement of the regional engorgement (Doorly et al., 2008b). The alteration of mucous layer and also the thickening of the mucous layer will change the surface structure of the nasal passageway and the effects of these changes has yet to be discussed in detail by previous works. In addition to that, models

implemented in FLUENT do not simulate the mucous lining, cilia or different epithelial surfaces as well as not replicating the changes in the nasal airway due to the nasal cycle during inhalation and exhalation (Kleven et al., 2005). These issues should be considered during analysis to get more accurate information regarding the factors effecting nasal airflow.

The inter-individual difference of the unique characteristic of nasal cavity becomes a crucial issue in the comparison of results among different researches (Croce et al., 2006, Riazuddin et al., 2011, Wen et al., 2007, Kelly et al., 2000). This study inspired from (Liu et al., 2009) encourages more standard nasal geometries to be created for different identifiable groups within the larger population. Therefore, this study is focused on creating a standardized model from a group of female Malaysians. Due to the asymmetric structure of nasal cavity, the standardized model was created based on both right and left nasal cavities. Lack of information on female nasal cavities has lead to the usage of this standardized model for the simulation as female nasal cavity is shorter in length as well as height compared to the male models (Riazuddin et al., 2011). (Jovanović et al., 2014) also stated that there were significant differences in the nasal parameters between male and female subjects. The standardized model characteristics such as cross sectional areas, velocity contours and the pressure drop were also analyzed. Varying the wide range of mass flow rate allows comparisons to be carried out for a detailed observation of the nasal airflow pattern caused by the increasing flow rates for both inspiration and expiration cases. Numerical simulation of the inspiration and expiration flow in the human nasal cavity performed by (Hörschler et al., 2003) was validated with experimental findings which used the same model. Thus, for this research, PIV experimental work is carried out using similar scaled up standardized geometry.



Validation is important for computational analysis to ensure the reliability of the results obtained.

The main purpose of the studies related to nasal cavities is to assist rhinologist in treatment planning and finding the best solutions for various disease cases. Sinusitis is a very common chronic illness with a substantial health impact and the factors contributing to sinusitis pathogenesis and its chronicity were reviewed by (Hamilos, 2000). Sinusitis was chosen to be studied in this research as it is a common disease in Malaysia. In addition to that, none of the previous researchers focused on the computational studies of sinusitis and therefore, leading to the lack of information available for such diseases especially the effects of pre and post-operational conditions. The relevance of whether surgeries should be carried out and to what extend the surgeries is helping the patient has not been analyzed. The expected outcome from this research is to prevent repetitive surgeries to be carried out on patients and therefore, reduce the financial burden as well as pain endured by the patients.

It is important to carry out this research as none of the previous works focuses on the female Malaysian nasal cavities. The standardized model created will be the first and only standardized model of female Malaysian which will serve as benchmark for pre and post-operational analysis. This new information obtained from the research will be a good addition to the literature.

### **1.3 – Aims and Objectives**

This research focuses in application of CFD in the study of human nasal airflow which is limited by the direct measurement methods. The main objectives for this research are listed as below:

- I.** To develop three-dimensional model of nasal cavity from CT scans and carry out numerical simulations to study the nasal airflow inside the nasal cavity.
- II.** To evaluate the effects of different thickness mucous layers on nasal airflow using CFD by comparisons with non-mucous layer model.
- III.** To develop a standardized adult female Malaysian's nasal cavity using averaging pixel values of CT scans and analyze the flow features in the standardized model via CFD simulations and comparisons with various models.
- IV.** To carry out computational simulations on pre and post-operational conditions on disease cases (sinusitis) and evaluate the effects of the surgeries performed on the patients.

### **1.4 – Scope of Work**

The scope of work for this research is based on the objectives as previously listed. The philosophy of this research revolves around application of CFD in the study of human nasal cavity and providing an advance step towards realization of virtual surgery. In order to implement virtual surgery into real cases, various preparations need to be carried out to ensure the reliability of this procedure and also to show the advantages of it compared to other procedures.

The first objective represents the general foundation for this research as it can be achieved by accomplishing other objectives as well. In order to carry out the study on human nasal cavity, data such as CT scan images were obtained from Advanced Medical and Dental Institute (AMDI), Kepala Batas with the help of rhinologist to identify the healthy and disease cases. Good collaboration between researcher and rhinologist are required throughout the whole research to obtain important explanation and information from the medical point of view.

The research is commenced with the development of three-dimensional female Malaysian nasal cavity for certain individual from CT scans by using several softwares such as MIMICS and CATIA V5 and then preceded with analysis carried out using FLUENT Software. Computational simulations on various thicknesses of mucous layers were carried out to study the effects of mucous layers toward nasal airflow as mentioned in the second objectives of this research. Results obtained from the simulation of the mucous layer effects were compared with non-mucous effects in order to solve the assumptions applied in previous researches related to mucous layer. This is to prove whether the assumption of mucous layer effects is negligible is applicable or not.

The third objective is to create a standardized female Malaysian nasal cavity that will be used as a control for the normal and healthy condition. Inter-individual geometrical differences of nasal cavity always become an issue as it is hard to compare the results obtained from previous works. CT scans of 26 healthy female nasal cavities within the age range of 20 – 45 years old were required for the generalization to obtain the standardized nasal cavity. Comparisons of four randomly chosen female nasal cavities with the standardized model were performed to proof that the standardized model is able to represent an averaged model of female

Malaysian nasal cavity. The comparisons were presented by examining the pressure drops, average velocity magnitudes and also cross sectional areas of all the models.

For this research, PIV experimental work for validation was carried out using 1:2.5 larger scales transparent mould of the standardized model manufactured made of Accura ClearVue Material using rapid prototyping method. Instead of utilizing air flow which is harder to control and set-up, mixture of water and glycerine was chosen as a replacement. Appropriate experimental set-up is required to imitate human inspiration flow. Clear images can only be obtained by suitable selection of seeding particles which involves the compromise of both the weight and also light scattering ability. The seeding particles must be light enough to be able to follow the flow but heavy enough to not float on the fluid, chemically inert to avoid any chemical reactions that will disturb the flow and able to scatter laser light in order for the movements to be captured by the camera. For a reliable validation, velocity vectors obtained from the experimental work were compared directly with the computational analysis of the similar standardized model. Results from acoustic measurements were also included for validation of computational simulations results of certain individuals.

The final objective deals with implementation of the standardized model as a benchmark for comparison which focuses on the study of pre and post-operational conditions on disease cases. Results comparisons with the standardized model allow better observation on the effects of the surgeries carried out. CT scans of both pre and post-operation of two patients with sinusitis (age 29 and 40 years old) obtained from Hospital Sultan Abdul Halim, Sungai Petani were used in the analysis. Three-dimensional model development and computational simulation were performed using similar methodology as the previous objectives. Velocity contours, average velocity

magnitudes, pressure drops and cross sectional areas of pre-operational were compared with post-operational cases to identify the successfulness and the relevance of the surgeries carried out on the patients. Besides that, in depth details on the effects of the surgeries towards curing the disease (sinusitis) can be investigated as well.

The existence of standardized model as a guideline will allow pre-operation conditions to be compared to the standardized healthy cases. These comparisons will be used to evaluate on how the surgeries should be performed in order to achieve the healthy condition. This step plays a very important role in turning the virtual surgery into reality and thus, assisting the rhinologist in decision making and also will be beneficial to patients of various disease cases.

## **1.5 – Thesis Organization**

This thesis is divided into five main chapters with inclusion of several sub chapters under the main chapters. The five main chapters consist of introduction, literature review, methodology, results and discussions and conclusion and future recommendations.

In the Chapter 1 – Introduction provides brief explanation on the research background, problem statement, and objectives with scope of work and thesis organization which is included to ensure readers are able to preview of the entire thesis. This is followed by Chapter 2 – Literature Review which represents the substantive findings of previous works that covers all the related topics and knowledge required for this research. Chapter 3 discusses the methodology of this research for both computational as well as experimental work. All the methodology

for computational analysis can be simplified into three parts which are pre-processing, running analysis and post-processing of results. In addition to that, experimental set-up was also described with the help of figures. Details explanation were presented on the development of three-dimensional nasal cavity from CT scans and also procedures involved in the creation of standardized model from 26 sets of CT scans. The most essential part of this thesis revolves around Chapter 4 covers both results and discussion. All the results obtained from the whole research were presented and compared with previous works. Results from computational analysis include various types of presentation such as tables, graphs and also mixture of images of the nasal cavities, contours and also streamlines. Any differences, changes and new findings were discussed and explained to proof the significance of the results obtained. Finally, the last chapter, Chapter 5 concludes the entire research and discusses on future recommendations for the improvement of this research.

## CHAPTER 2 – LITERATURE REVIEW

### 2.1 – Nasal Anatomy

Human respiratory system which includes nasal airways, lungs and the respiratory muscles plays an important role for respiration which includes inspiration and respiration, as it carries respiratory gaseous in and out of the body. Human nasal cavity becomes the main focus in this study as it is the first area to be in contact with outside air during normal healthy respiration. Human nasal anatomy and physiology are briefly discussed in this section.

#### *2.1.1 Nasal Structures and Functions*

Human nasal airway is a complicated structure covering the areas starting from the nostrils up to the nasopharynx as shown in **Figure 2.1**. Adult human nasal cavity is approximately 7.5 cm long (measured from anterior nares up to posterior nares) and 5 cm high (measured from the base of inferior meatus until olfactory slit) (Kerr et al., 1987). The nasal cavity is not only acts as a passageway for air but also responsible for smelling as well as filtering, warming and humidification of the inspired air. Normally nasal cavity is used for resting breathing while mouth breathing is used during active or extreme breathing which requires increase in the volume of airflow by opening the mouth (Hunt et al., 2008, Lane, 2004).

The human nasal cavity consists of two symmetrically complex three-dimensional nasal passages that are separated in the middle by the nasal septum starting from nostrils until the end of turbinates (Zubair, 2012). The unique characteristics of nasal cavity cause it to differ individually. However, the main structures can be summarized generally as air flows into the upper respiratory system

via the nostrils during inspiration and then reaches the smallest cross-sectional area, the nasal valve before reaching the tortuous turbinates region that forms large cross sectional areas covered with mucous layers and cilia. Finally, the air will enter the lower respiratory system via nasopharynx. During expiration, the air will go through the opposite pathways starting from nasopharynx towards the nostrils.

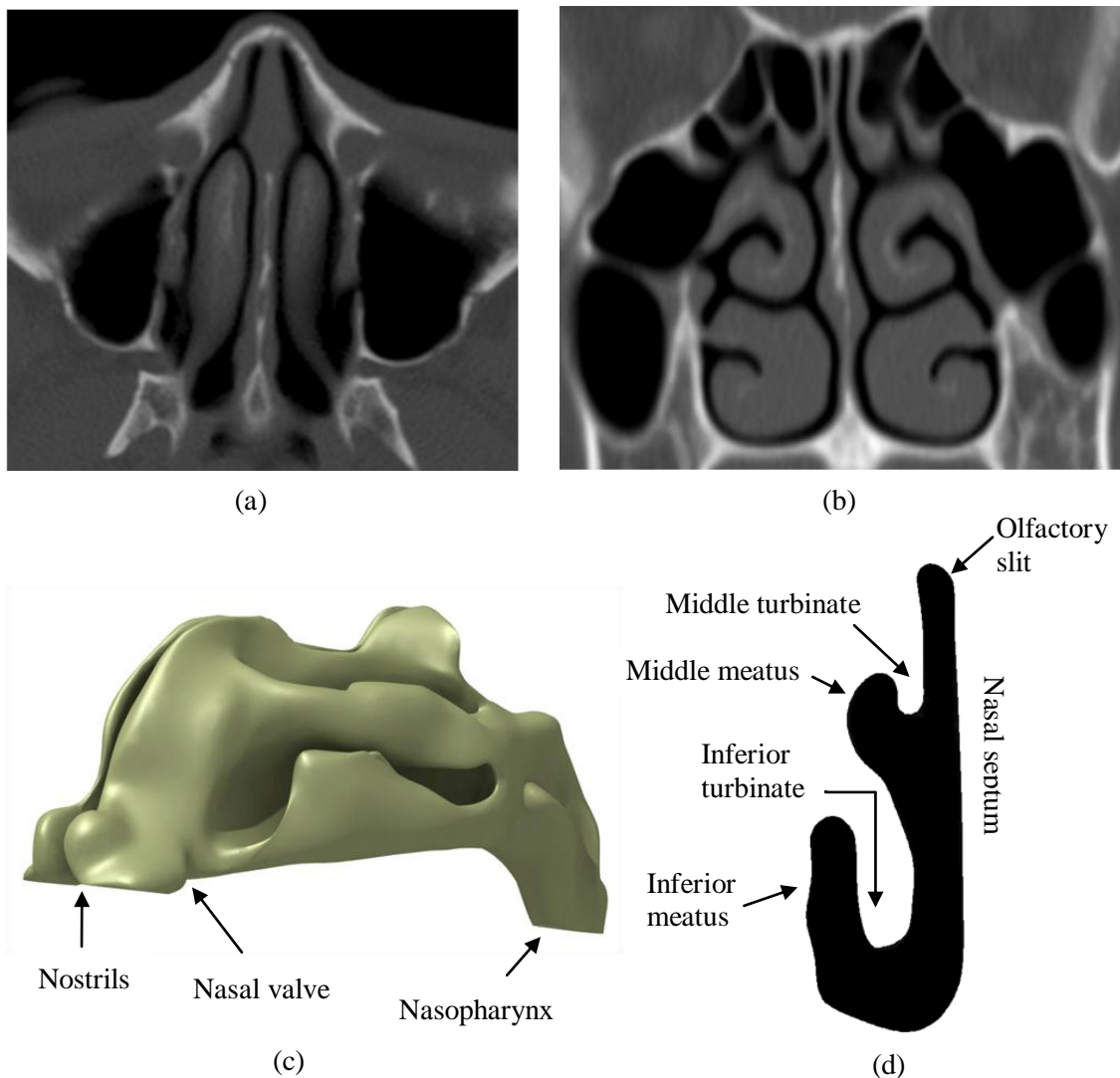


Figure 2.1: Nose anatomy (a) CT scan - Axial view, (b) CT scan – Coronal view, (c) 3D view of nasal cavity and (d) Half nasal cavity with labels

Nostrils (or external nares) are located at the most outside part of the nasal cavity where it is the first part of upper respiratory system to be in contact with



outside air. Nasal vestibule is located slightly posterior to the nostrils. The shape and size of vestibule varies according to individuals, genders, ages as well as races. Vestibules are easily exposed to harmful airborne particles during inspiration and thus, it is covered by skin which is made of stratified squamous epithelium and also nasal hair follicles (Rajagopal and Paul, 2005). Hazardous airborne particles will be filtered by the nasal hair follicles and sebaceous glands (Chometon et al., Liu et al., 2009). Vestibule is demarcated from the tortuous meatuses in the inner nasal cavity by the nasal valve. Nasal valve is the smallest cross-sectional area and is usually located around 2 to 3 cm from the anterior tip of the nose (Wen et al., 2007). Nasal valve accounts for highest nasal resistance and any abnormalities in this region will definitely cause major nasal obstruction (Walsh and Kern, 2006).

Left and right nasal cavities are separated by a partition of bone and cartilage covered by respiratory mucous layer called nasal septum. Nasal septum is an important structure which provides support for the structure of the nose and also influences the intranasal airflow pattern (Polat and Dostbil, 2009, Walsh and Kern, 2006). Other than that, nasal septum also contributes in conditioning and humidification of the inspired air to make it more suitable for lower respiratory system (Polat and Dostbil, 2009, Simmen et al., 1999). Study was carried out by (Simmen et al., 1999) to evaluate the nasal airflow characteristics and to examine the effect of structural changes of nasal septum and turbinates. Deviated nasal septum (DNS) due to asymmetric nasal cavities is commonly observed in patients complaining about nasal discomforts such as obstruction of stuffiness (Kim et al., 2010).

The tortuous region of the nasal cavity consist inferior, middle and superior turbinates which responsible for heat exchange, humidification and as aerodynamic

guides of the inhaled air (Chometon et al.). Meatuses are the air passageway defined by the turbinates, for example inferior meatus is located under the inferior turbinate. The inferior turbinate, located at the floor of nasal cavity is the largest compared to middle and superior turbinate. It is subject to considerable variation in size due to the changes in its sub-mucosal vascular bed (Kerr et al., 1987). Inferior meatus with wide airway results in drying of the mucous layer and crusting. Partial inferior turbinectomy is usually performed on the patients suffering from chronic nasal obstruction due to hypertrophy of inferior turbinates (Chen et al., 2009). Middle turbinate, similar to inferior turbinate, is subject to variations in shape and size. Middle meatus plays an important role as the main drainage passageway for the sinuses and most likely to identify the evidence of sinus diseases (Kerr et al., 1987). The superior turbinate is a vestigial remnant and a small structure of the nose which is difficult to identify and is usually omitted in studies because the airflow in the region is considered very small (Elad et al., 1993, Doorly et al., 2008b, Hörschler et al., 2006, Lee et al., 2013, Naftali et al., 1998). Superior turbinate is absent in more than 80% of the population (Naftali et al., 2005). After entering the separate passageways at the turbinates, the airflow increases in velocity and rejoined in the nasopharynx, where the airflow changes direction for entering the lower respiration system (Hunt et al., 2008, Kleven et al., 2005).

The paranasal sinuses are four pairs of hollow structures within the bones that surround the nose as shown in **Figure 2.2** (Kunkel et al., 2009). The maxillary sinus is the pneumatized space within the maxillary bone and is the largest among the paranasal sinuses (Walsh and Kern, 2006). The ethmoidal sinus consists of a complex system of air-filled cells located in the lateral nasal wall and are divided into anterior and posterior cells by the middle lamella in the middle concha (Wagenmann

and Naclerio, 1992). Meanwhile, the frontal sinus in the frontal bones is asymmetric and varies widely in size and extension (Wagenmann and Naclerio, 1992). The sphenoid sinus is located below the pituitary fossa, and its lateral aspect is formed by the cavernous venous sinuses (Slavin, 1984).

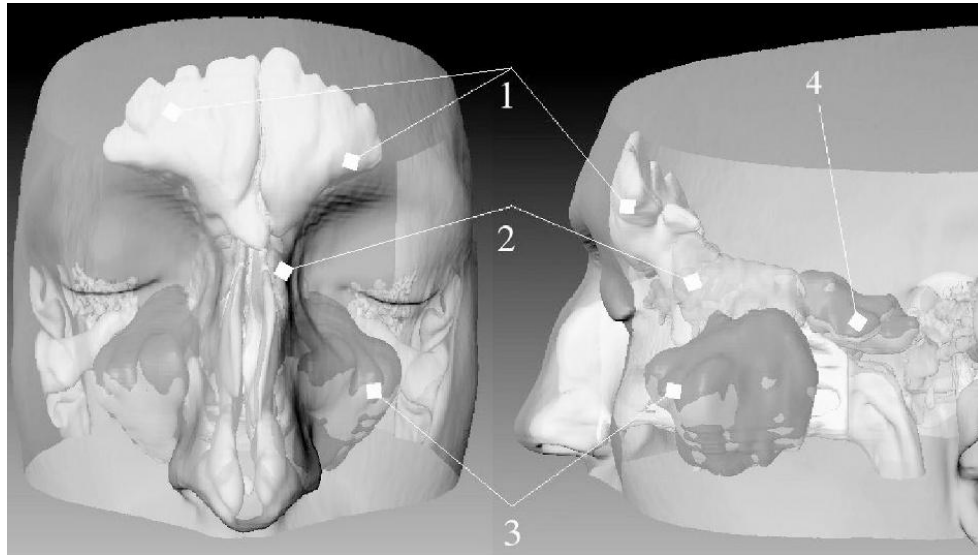


Figure 2.2 : Human paranasal sinuses: (1) Frontal, (2) Ethmoidal, (3) Maxillary and (4) Sphenoidal (Figure obtained from (Kunkel et al., 2009))

## 2.2– Mucous and Related Fields

Mucous layer is a single homogenous and thin mucous film covering the outer surface of nasal hair follicles (also called vibrissae) that is important to warm, humidify and to clean the inspired air with the help of nasal mucociliary action supported with the nasal hair (Garcia et al., 2007a, Doorly et al., 2008a). Mucous layer has become a field of interest for research such as detailed investigations on its compositions, structures and also its characteristics.

### ***2.2.1 Mucous Characteristics and Structures***

Mucous layer is described as a superficial watery layer and is estimated to be 5 to 30  $\mu\text{m}$  thickness (Kurtz et al., 2004). Mucous lining along the airway luminal surface plays a very important defensive role against airborne particles and chemical, thus acts as human's essential first line of defence against infections (Mukherjee, 1977, Chantler and Ratcliffe, 1988). Mucous layer also serves as a barrier that controls the absorption of gases and drugs into the walls of the conducting airways (Tian and Longest, 2009). Atrophic rhinitis is a chronic disease of the nasal mucosa and as mentioned by (Garcia et al., 2007a, Garcia et al., 2007b), this disease is caused by excessive evaporation of the mucous layer. Recently, (Mosges et al., 2009) conducted an investigation to three-dimensionally visualize the spatial distribution of mucosal swelling in the nasal cavity to demonstrate the protective effects of Mometasone furoate nasal spray (MFNS) on exposure to allergens. (Hemtiwakorn et al., 2009) stated that the factors of cilia, mucous lining and epithelial tissues being ignored in the analysis and proposed that, in order to ensure accurate numerical simulation of fluid shear stresses, e.g. changes of air velocity at the mucosal wall, several dense layers of pentahedral prism elements at the air mucosa interface should be introduced in future studies. In addition, (Tian and Longest, 2009) and (Chometon et al., 2001) also considered mucous layer in their researches by incorporating 10  $\mu\text{m}$  as the mucous layer thickness. Meanwhile, (Getchell et al., 1984) stated that mucus was described as consisting of a superficial watery layer estimated to be 5  $\mu\text{m}$  thick and a deeper, more viscous layer estimated to be 30  $\mu\text{m}$  thick. (Wagenmann and Naclerio, 1992) mentioned that the nasal mucosa covers up to 100 to 200  $\text{cm}^2$  of surface area, the mucous layer is 10 to 15  $\mu\text{m}$  thick and is continuously moved by the cilia at a speed of 6 mm/min. (Zhao et al., 2004), (Xiong et al., 2008) and (Zachow et

al., 2009) have concluded that relatively small changes in the anatomy of nasal cavity at specific locations may effectively alter the airflow distribution and thus can induce large change in the nasal airflow.

The essential structural element of mucous is glycoprotein, formed from a protein core surrounded by carbohydrate side chains, which accounts for over 70% (by weight) of the molecule (Schipper et al., 1991). The presence of glycoprotein gives the mucus its gel-like structure. Optimum function of mucus is performed when individual components are present in proper concentrations and pathology may occur when the optimum function of mucus is distorted due to altered quality of its individual components (Lillehoj and Kim, 2002). The lateral walls of the nasal cavities is irregular and carries bone plates covered with an erectile mucous membrane, which spreads out to the back of the nasal cavities, thus dividing the respiratory flow (Croce et al., 2006). Its functions are to protect the entry of the sinuses and to increase the surface area of exchange for inspired air while maintaining the narrow shape of the cavity (Croce et al., 2006). The region of the turbinates is covered with pseudo-stratified columnar and ciliated epithelium, the lamina propria, supplement the secretion of the goblet cells and veins in the lamina propria form the thin walled, cavernous sinusoids, also called cavernous bodies as observed in **Figure 2.3** (Elad et al., 2008, Slomianka, 2006).

Mucous layer also serves as a barrier that controls the absorption of gases and drugs into the walls of the conducting airways (Tian and Longest, 2009). (Naftali et al., 1998) also recommended a more detailed study on the descriptions of the dynamics processes of heat, water and soluble gas transfer at the mucosal surface. Exposure to formaldehyde causes a slow clearance in the anterior nose and changes in nasal mucosa that may lead to an inhibitory action on the mucociliary function of

the nasal mucosa which in turn is responsible for the development of chronic rhinitis and sinusitis (Proctor and Baltimore, 1983, Sherwani et al., 2002, Franks, 2005). (Barton and Raynor, 1967) has investigated the effects of mucous density, viscosity and layer depth on the flow phenomena. The effects of cilia diameter, length, spacing and oscillation frequency are determined from equations governing the flow of the mucous blanket. The nasal cavity is covered with a thin film of mucous layer which is also important for warming and humidifying inspired air. Lack of humidification will cause dryness and crusting that will lead to various diseases and cause difficulties to patients (Garcia et al., 2007a).

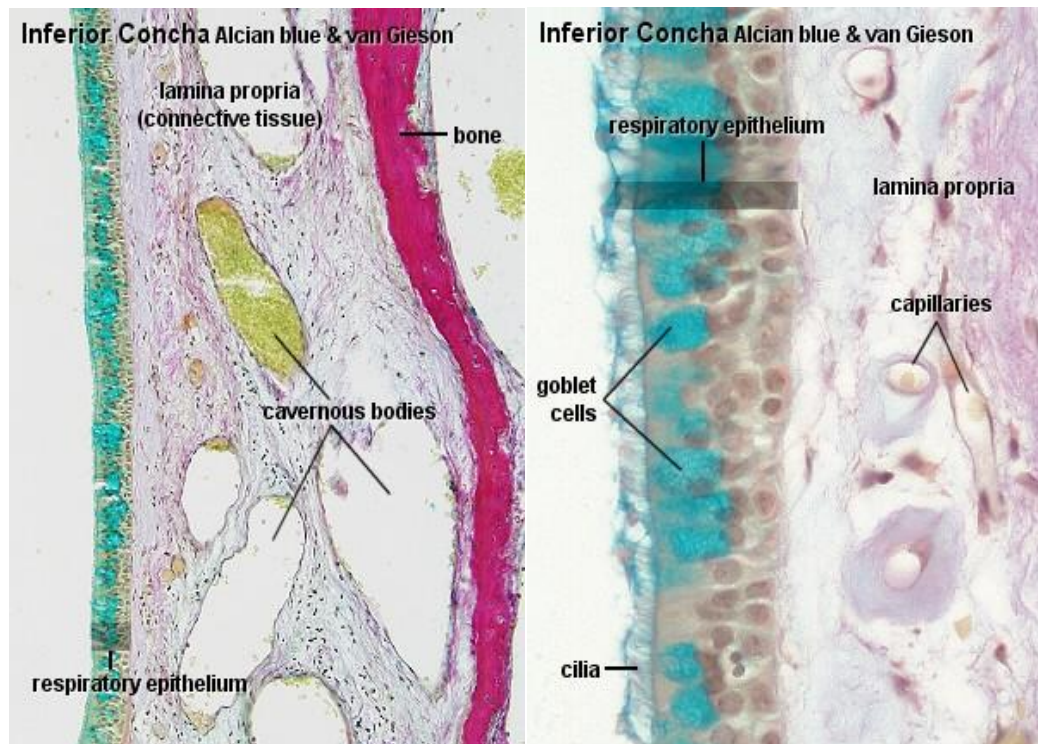


Figure 2.3: Ultrastructure of the nasal wall at the respiratory region that shows the pseudo-stratified columnar and ciliated epithelium, the mucus producing goblet cells, the lamina propria, the mucous and serous glands and the cavernous sinusoids (Figures obtained from (Elad et al., 2008) and (Slomianka, 2006))

### ***2.2.2 Nasal Mucociliary Clearance***

Nasal mucociliary clearance can be divided into two fundamental units which are the mucus and cilia, both involved in the physiological process which allows mucus to flow over an epithelial lamina of ciliated cells. It represents the first defensive barrier against biological and physical insults in nasal fossae, paranasal sinuses and inferior respiratory tract (Passali et al., 1999, Polat and Dostbil, 2009). This defence system is mainly due to the viscoelastic properties of the mucus which will entrap nearly all the particles that are larger than 5  $\mu\text{m}$  and more than 50% of particles that range from 2-4  $\mu\text{m}$ ; and by using nasal mucociliary action to push the particles towards pharynx so that they can be swallowed or expectorated within 15 minutes to be clear out from human body (Taylor et al., 2009, Wolf et al., 2004). This process will eliminate all the harmful particles that go into the respiratory tract.

Thus, in order to detect the nasal mucociliary clearance time, a standard saccharine test was used. Saccharine test was performed in a sitting position where approximately 0.5 mm particles of saccharin were placed 1 cm behind the anterior end of the inferior turbinate and the time is recorded. In order to obtain reliable results, subjects were instructed to breathe through the nose normally and were told not to sniff, sneeze, eat or drink. Then, the subjects were instructed to notify the first definite sweet taste sensation (Pandya and Tiwari, 2006, Yadav et al., 2001, Golhar and Arora, 1981, Yadav et al., 2003, Barry et al., 1997, Deniz et al., 2006). These studies were carried out to determine the nasal mucociliary clearance time of normal subjects compared to subjects with various sino-nasal pathologies such as rhinitis, atrophic rhinitis, patients with tracheostomy and also total laryngectomized patients (Pandya and Tiwari, 2006, Yadav et al., 2003, Deniz et al., 2006). Besides the saccharine test, mucociliary transport rate can also be determined using a

<sup>99m</sup>Tc sulphur colloid drop deposited on the nasal mucosa of one nostril. Any influence of gravity on the drop motion over mucosa is avoided by positioning the head lateral under a gamma-camera (Pavi et al., 1987, Polat and Dostbil, 2009, Kaya et al., 1984). The <sup>99m</sup>Tc-labelled resin particles are chosen because of its optimal physical characteristics of the radioisotope, ease in labelling, stability of the label and the chemical inertness of the resin particles (Kaya et al., 1984). Mucous layer under the effect of mucociliary moves towards the nasopharynx at a speed of 4-6 mm/min, at relatively low speed of the mucociliary, smooth no-slip and perfectly absorbing boundary conditions are reasonable assumptions for analysis (Shi et al., 2006). The study on nasal mucociliary clearance have also been widely discussed especially when it is related to the optimization of drug administration. This is due to the nasal mucosa having a large surface area and also very vascular, therefore this enables an effective drug absorption when compared to gastrointestinal mucosa (Schipper et al., 1991).

### **2.3– Computational Analysis**

The availability of advanced imaging techniques such as CT scans and MRI provides better visualization of the nasal geometry. However, these imaging techniques have their limitation in obtaining vital information such as airflow patterns, velocity, pressure changes and nasal resistance along the nasal cavity (Riazuddin et al., 2011, Zubair, 2012). This leads to the advancement of the studies with the usage of computational analysis where the nasal cavities can be depicted exactly from the human model and used in computational analysis to view the airflow pattern along the nasal cavity (Weinhold and Mlynski, 2003, Lee et al., 2012b).



### ***2.3.1 Geometrical Modelling***

Generally, researchers used identical models as shown in **Figure 2.4(a)** as they replicate the exact structures of the nasal passageway, with only slight modifications to the structures for simplification purposes. The models that fully replicate the internal and external nasal airways of two anatomically distinct subjects were used to study nasal airflow and the results obtained were compared with experimental observations to determine the accuracy of the analysis (Taylor et al., 2009). Entire nose from the nasal tip to the posterior wall of the nasopharynx should be used for analysis because if these extremes are not included, then the effect of the nostrils during inspiration and the effect of the nasopharynx in directing the airflow downward will not be modeled and thus leading to a potentially unrealistic representation of the nasal airflow (Bailie et al., 2006).

Geometrical models varied with the type of studies performed. Therefore, models from a healthy human who does not possess any obvious pathological symptoms and vice versa are required for a better understanding and visualization of a normal nasal airflow (Lee et al., 2010, Taylor et al., 2009, Ishikawa et al., 2006, Zachow et al., 2007, Inthavong et al., 2007, Zhao et al., 2004). For example, Garcia et al. conducted a research using CT scans of a patient with primary atrophic rhinitis (Garcia et al., 2007a, Garcia et al., 2007b). This allows different conditions especially on patients with chronic diseases to be analyzed and obtain more information in providing improved treatments for such cases. Furthermore, (Croce et al., 2006) used a realistic plastinated human model which is anatomically conserved with left and right nasal cavities for experimental purposes. This model was scanned to obtain CT images for specific three-dimensional reconstruction procedures that

were implemented for numerical simulations. Results from both models were compared for validation purposes to ensure the accuracy of the analysis.

In order to avoid discrepancies in the results obtained, some researchers made modifications to the nasal cavity. A study on nano-particle or vapour deposition which was carried out by (Shi et al., 2006) required not only the typical anatomical model but also some additional geometry as shown in **Figure 2.4(b)**. A short inlet tube was added to the nostril to prevent simple plug flow from entering the nostrils and a certain length of actual airway was added to the nasopharynx to obtain proper outlet conditions. (Zachow et al., 2006) used highly detailed anatomy of a nasal airway which included frontal and paranasal sinuses in the airflow simulations. (Kunkel et al., 2009) evaluated an approach for the use of segmented CT images in volumetric estimation of the paranasal sinuses cavities. The results show accurate comparisons between the volume estimation of paranasal sinuses from an anatomical model by material injection and by 3D reconstruction of CT images (Kunkel et al., 2009). Meanwhile, (Leung et al., 2007) discussed how the shape and size of the nose affects the airflow pattern inside the nasal cavity. The geometry of the nasal cavity model is derived from both spiral and cone beam CT scans for comparison and the results concluded that there are no significant differences between both models. Therefore, cone beam CT imaging is said to be a better choice because of its less radiation dose and able to provide high contrasting images in hard as well as dense tissue (Leung et al., 2007). All these methods are adopted to create an anatomically identical model which considers all the details to be able to replicate an actual nasal cavity.

Meanwhile, **Figure 2.4(c)** proposed a nose-like model, which was a simplified model of the human nose by using the average data of human nasal cavities (Elad et al., 2008). The superior turbinate was omitted because lack of airflow in this region. This generalize nose-like model is a simplified version to the complex structure of the three-dimensional nasal cavities and allows removal or addition of various features to the model. These changes are very useful so that different types of comprehensive analysis can be carried out with ease (Naftali et al., 1998). For analysis of air-conditioning capacity, the nose-like model was able to yield similar results to the anatomical model (Naftali et al., 2005). (Hörschler et al., 2006) investigated the impact of the geometry on the nasal airflow by using different models of human nasal cavity with and without turbinates. Both computational and experimental works are carried out and show a convincing agreement at both inspiration and also expiration as far as the flow topology in several sagittal and coronal cross sections is concerned. Importance of turbinates were explained in details as it serve as a guide vanes to ensure a homogenous velocity distribution in the lower, middle and upper channel between the nostril and the throat (Hörschler et al., 2006).

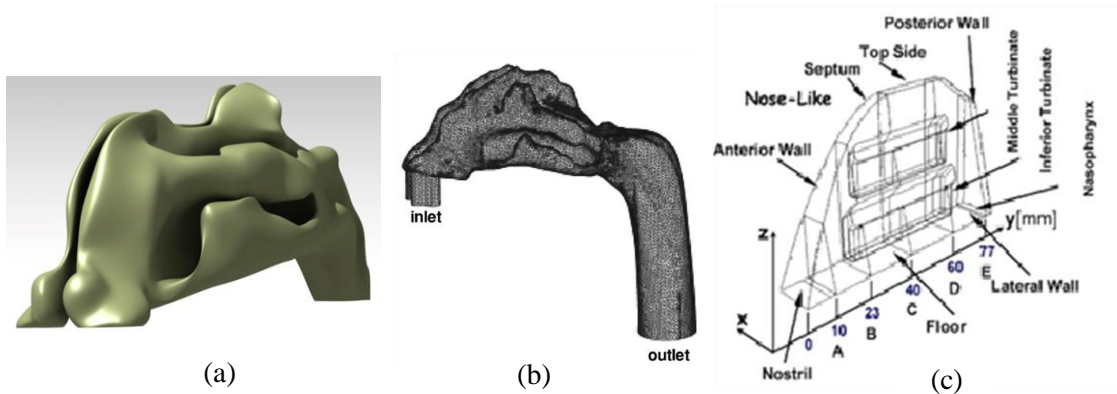


Figure 2.4: Models of the nasal cavity (a) Anatomically identical model, (b) Nasal cavity with additional inlet tube and extended nasopharynx, and (c) Simplified nose-like model (Figures obtained from (Shi et al., 2006) and (Elad et al., 2008))

Differences in nasal anatomy among human subjects may cause significant differences in respiratory airflow patterns and subsequent dosimetry of inhaled gases and particles in the respiratory tract. (Segal et al., 2008) used CFD to study the inter-individual differences in nasal airflow among four healthy individuals and the results show the flow differences do exist among different individuals. (Liu et al., 2009) has summarized geometric characteristics of the nasal cavities of 30 healthy adults; to develop an objective methodology for aligning, scaling and averaging the associated 60 single individual nasal passages; and to use this methodology to create a single, detailed, standardized geometry that could be considered as a standard human nasal cavity for aerosol deposition studies (experimental and numerical).

### ***2.3.2 Advantages of Computational Simulations***

Diverse approaches implemented to study nasal airflow including experimental, computational and objective measurement techniques. Objective measurement methods are very common in studies related to nasal geometry where it is used to determine cross sectional area, nasal airway resistance and also for visualization of the human nose. (Suzina et al., 2003) used active anterior rhinomanometry (AAR) for objective assessment of the nasal airway resistance in normal adult Malays. (Shelton and Eiser, 1992) carried out an evaluation of active anterior and posterior rhinomanometry in normal subjects. However, these methods have its limitation in measuring the precise velocity of the airflow and in evaluating the local nasal resistance in every portion of the nasal cavities (Ishikawa et al., 2006). In addition to that, the complex nasal anatomy consists of numerous thin airway